JOURNAL OF AIRCRAFT
Vol. 50, No. 3, May–June 2013

Separation Dynamics of Air-to-Air Missile Using a Grid-Free Euler Solver

K. Anandhanarayanan,* Konark Arora,† Vaibhav Shah,†
R. Krishnamurthy,† and Debasis Chakraborty†
Defence Research and Development Laboratory, Kanchanbagh, Hyderabad, India

DOI: 10.2514/1.C031791

The study of separation dynamics of a missile from a fighter aircraft is a prime requirement to ensure the safety of the aircraft before flight testing the missile. An integrated store-separation-dynamics suite has been developed and applied to study the separation of an air-to-air missile from a fighter aircraft. The suite consists of a preprocessor to generate connectivity using overlapped unstructured grids, a three-dimensional grid-free Euler solver to obtain aerodynamic forces and moments on the missile and a six-degrees-of-freedom solver to integrate the equations of motion. A quasi-steady approach has been used to simulate the separation dynamic of rail-launched missile. The motion of the missile guided by the rail launcher has been modeled using constrained-force method and implemented in the six-degrees-of-freedom code. The surface transpiration boundary condition has been incorporated in the Euler solver to mimic the aerodynamic damping and the relative motion of the missile with respect to the aircraft. The store-separation-dynamics suite has been applied to obtain the trajectory of the missile at various aircraft launch-envelope conditions.

I. Introduction

CONFIRMING the safe separation of an air-to-air missile from a fighter aircraft is a daunting and obligatory task. The separation characteristics of a missile can be obtained using flight testing [1], experimental techniques such as captive trajectory system (CTS) [2], and computational methods using Cartesian grids [3], chimera grids [4], or combined moving and remeshing methods [5]. The flight testing is more accurate but very expensive and risky for a newly designed weapon system before characterizing using experimental or computational methods. Recently, due to the advent of powerful computers and efficient algorithms, the computational fluid dynamics (CFD) is used as a main tool to obtain separation characteristics in the design cycle, and finally, the CTS is used to confirm the design using online method [6] and generating a large aerodynamic database of separating missiles using grid method [7] for parametric-variation studies. The chimera-grid method is powerful in handling multibody simulations, but it has some limitations such as difficulty in modeling thin gaps and interpolation in the flow-discontinuity regions. The grid-free methods [8–11] do not have the above difficulty because there is no interpolation involved as in chimera-grid methods and further, grid-free methods are simpler for implementing implicit methods and parallelization of grid-free code due to uniform treatment at all the points. A grid-free Euler solver based on entropy (q) variables least-squares kinetic upwind method (q-LSKUM) has been developed [12]. The grid-free solver requires a cloud of points around the configuration and a set of neighbors (connectivity) around each point. Unstructured grids around fighter aircraft and missiles are generated independently, and then these grids are overlapped to get the distribution of points around the full configuration. An efficient preprocessor [13] has been developed and applied to generate the connectivity. Parallel version of three-dimensional grid-free Euler solver q-LSKUM has been used to obtain the aerodynamic characteristics of the aerospace vehicle configuration. The solver has been verified and validated for axi-symmetric and wing-body missile configurations. The solver has been applied to a large number of aerospace multibody problems [14]. A six-degrees-of-freedom (6-DOF) solver has been integrated to the Euler solver along with the preprocessor to form a store-separation-dynamics suite. The integrated suite has been validated for a generic store separating from a wing [15]. The suite has been applied to the aircraft-missile configuration to obtain the captive loads of the missiles [16]. In the present study, the suite has been applied to obtain separation characteristics of the missile from the fighter aircraft.

Received 19 December 2011; revision received 0 ; accepted for publication 17 October 2012; published online 7 March 2013.

*Directorate of Computational Dynamics; kanand_cfd@yahoo.com, anandha@drdl.drdo.in (Corresponding Author).
†Directorate of Computational Dynamics.

II. Grid-Free Euler Solver

The least-squares kinetic upwind method (LSKUM) [17] is based on the kinetic-flux-vector-splitting [18] scheme, which exploits the connection between the Boltzmann equation of kinetic theory of gases and the governing equations of fluid dynamics using a moment-method strategy. More specifically, Euler equations are obtained by taking Ψ-moments of the Boltzmann equation with Maxwellian velocity distribution function. In LSKUM, the spatial derivatives of the Boltzmann equation are discretised using a weighted least-squares method. The connectivity is split into substencils based on the sign of molecular velocity to evaluate the spatial derivatives that satisfies the upwind property, and finally, taking Ψ-moments leads to the LSKUM numerical scheme. The higher-order accuracy in space is achieved using a defect-correction method [19] in which the lower-order spatial errors are removed using an iterative strategy to get the desired spatial accuracy. An improved version of LSKUM is q-LSKUM [20] in which the entropy variables, also called q-variables, are used in the defect-correction step to achieve the higher-order accuracy in space at all points including boundary points. The wall boundary point is treated using kinetic characteristic boundary condition [21] to impose the slip wall boundary condition. The far-field boundaries are treated using kinetic outer boundary condition (KOBC) [21] without reflecting any outgoing waves. This boundary condition is applicable for both inflow and outflow boundaries in subsonic and supersonic flows. The aircraft intake is also treated using KOBC to simulate the flow through intake. This treatment avoids modeling the complex flow through the aircraft engine or presence of normal shock ahead of closed air intake. The convergence acceleration device lower-upper symmetric gauss seidel has been developed in the grid-free LSKUM framework [22] and implemented in the q-LSKUM Euler solver. Further, the solver has been parallelized using message passing interface to work on the distributed-memory computing systems [23]. The only geometric entity is point in the grid-free

method and therefore, implementing implicit methods and parallelization of the q-LSKUM solver are straightforward even for very complex and relatively moving multibodies. The simulations involve subsonic, transonic and supersonic flows past flight vehicles. The aerodynamic forces consist of pressure and skin-friction components. The Euler solver predicts the pressure forces accurately. However, the skin-friction force is obtained using van Driest method assuming that the surface values as boundary-layer edge conditions [24]. The skin friction along with the surface pressure is integrated to get the aerodynamic forces and moments.

III. Generation of Data Structure

The grid-free solver requires just a distribution of points and a set of neighbors, called connectivity, around each point. The distribution of points can be obtained by two methods, namely simple-cloud method and chimera-cloud method. In simple-cloud method, the point distribution is obtained using the grid around the body and leaving the grid lines. In chimera-cloud method, the complex geometry is subdivided into geometrically simpler shapes and clouds of points are generated around the individual components. The simple clouds are then overlapped to get the distribution of points over the entire computational domain. The chimera-cloud method basically uses grids to get the distribution of points and connectivity, but the present method is efficient compared to the chimera-grid method. An efficient preprocessor [12] has been developed to generate the connectivity using overlapped structured grids and recently the preprocessor has been extended to generate the connectivity using overlapped unstructured grids [14]. The preprocessor accepts multiple unstructured grids and overlaps the unstructured grids as per the geometry position. The neighbors of the nodes are obtained using the edge connectivity information of the grid. Due to overlapping of multiple grids, certain nodes of one grid may fall inside other components, and these nodes should be removed or blanked. There are some cells of one grid may be cut by the surface of other grid. The nodes of such cells which lie inside the geometry are blanked and the outside nodes are retained for the computations. But the connectivity of such outside nodes should contain nodes from the same side of the cutting surface. Therefore, the nodes that are either inside the component or on the opposite side of the surfaces are removed from the connectivity. Further, the connectivity of such nodes is updated by adding more supporting nodes from the overlapping grids. The supporting nodes from overlapping grids are obtained using a gradient-search algorithm [25].

In the present study, the geometry consists of fighter aircraft with four missiles, which are placed at two different locations on either side of the wing as shown in Fig. 1. The missile is initially guided by the rail launcher and three launch shoes as shown in Fig. 2. The unstructured grids are generated around aircraft and missile geometries. The grids are then overlapped to get chimera clouds of points and the preprocessor is applied on these clouds of points to blank the solid points and to generate the connectivity for each point. The sectional grids in pitch plane of aircraft and missiles are shown in Fig. 3. The details of the geometry, grid generation, and connectivity generation are given in [16].

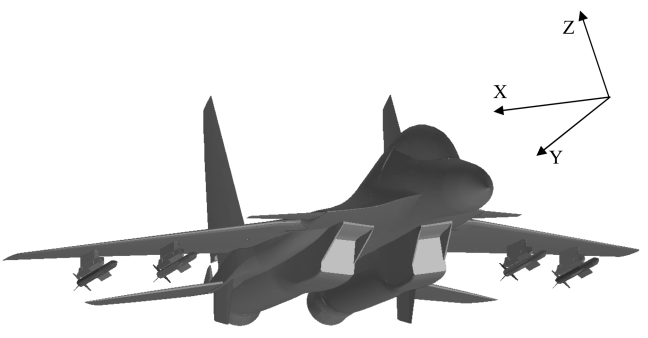

Fig. 1 Isometric view of fighter aircraft with missiles.

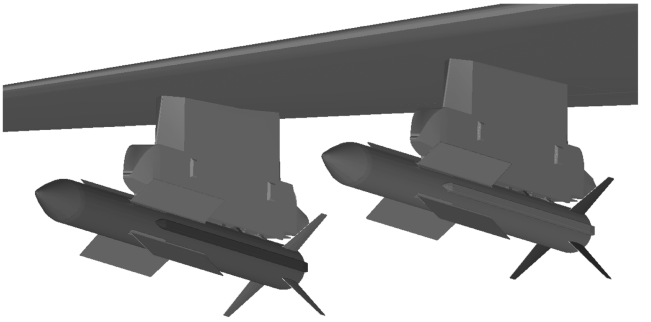

Fig. 2 Missiles integrated to the wing of fighter aircraft.

IV. Trajectory Simulation

The store relative motion with respect to the launching aircraft is obtained using a 6-DOF solver. The equations of motion are solved in the missile-body frame, whereas the aerodynamic simulation is carried out in the inertial frame that is attached to the nonmanuvering aircraft. The integrated simulation involves the repeated transformation of various vectors such as force, moment, velocity, and displacement from one frame to another. These transformations of vectors are carried out using quaternion. The simulations are carried out for powered, rail-guided air-to-air missiles. The first phase of the separation is along the rail constrained by three launch shoes present in the missile. The second phase is tip-off motion; that is the condition when the first two shoes leave the launcher but the third shoe alone is in contact with the rail of the launcher. After the third shoe also comes out of the launcher, the missile has all the six degrees-of-freedom motion in the third phase. The constraint-force method is used to obtain the reaction forces during the first two phases. These reaction forces are used to constrain the motion of the missile and to verify the structural integrity of the launch shoes with missile and rail launcher with aircraft. The thrust history is considered along with aerodynamic and launch-shoe reaction forces to simulate the motion of the missile. The changes in mass, moment of inertia, and centre of gravity (cg) of the missile are also considered in the simulation. The instantaneous missile attitude is used to rotate the missile grid about the missile cg. Therefore, three equations for the translation of missile cg are also solved along with other equations in the 6-DOF solver.

V. Modeling of Aerodynamic Damping

The store-separation study has been carried out using a quasi-steady approach. The grid-free Euler solver is applied on the chimera cloud of points to get the aerodynamic loads on the missile

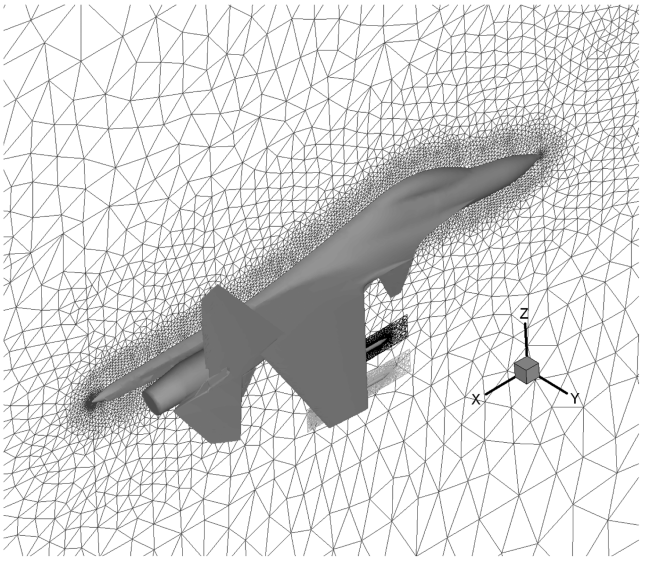

Fig. 3 Grids on symmetry planes of fighter aircraft and missiles.

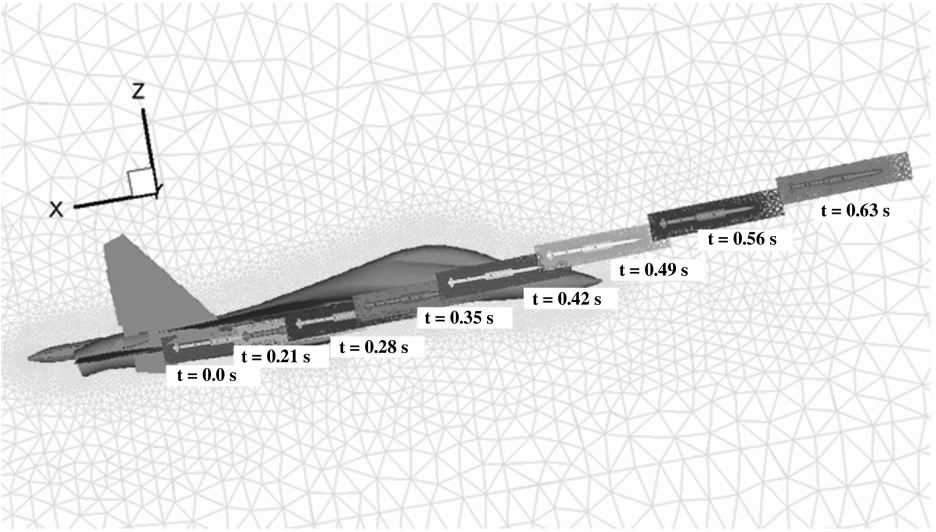

Fig. 4 Grids on symmetry planes of fighter aircraft and missile during separation.

configuration. The loads are integrated using a 6-DOF solver to obtain the velocity and position of the missile. The unstructured grid around the missile is moved to a new location and the preprocessor is applied to get a new set of cloud of points. This procedure is continued until the store reaches the safe distance. The overlapped grids at various time instants are shown in Fig. 4. Should there be any interference, the preprocessor during blanking of solid points, indicate the interference and terminates the computation with error message. In the quasi-steady approach, a steady-state flow solution is obtained with flow-tangency boundary condition applied on the surface of the store and aircraft at each time step. This approach does not consider the motion of the store relative to the parent aircraft. This model fails to address the induced incidence experienced by the store due to the body motion and the aerodynamic damping due to the angular motion of the store. Unsteady flow simulation is required to model these dynamic effects, but at the cost of increased computer run times. Therefore, an intermediate approach is followed in the present work to model the dynamics. This approach models the motion of the store relative to the parent aircraft via transpiration boundary condition [26] applied on the surface of the store. The transpiration boundary condition models the relative movement by imposing a flow in or out at each boundary node on the surface of the store to match the linear and angular velocity of that point on the store relative to the parent aircraft. Because the motion of the store relative to its parent aircraft is modeled by this technique, the effects of the induced incidence and damping due to rotary motion are also modeled. This boundary condition is implemented in the CFD solver to account for the aerodynamic damping of the air-launched missile.

VI. Results and Discussion

The overlapped cloud of points is generated around the aircraft and missiles. Then, the grid-free q-LSKUM Euler solver is applied on the cloud of points to estimate aerodynamic loads on aircraft and missiles. The diameter and base area of the missile are considered as the reference length and the reference area for the missile loads. Similarly, the mean aerodynamic chord and surface area of the wing are considered as the reference length and the reference area for the aircraft force and moments. The simulations have been carried out on a Linux cluster using 100 nodes of Intel dual Xeon at 3.8 GHz with 4 GB RAM processor. Various numerical experiments have been carried out to select the parameters to get the trajectory with reasonable accuracy and minimum possible time. The grid-dependence study and the intercode comparison have been made for the aircraft and missile configuration during estimation of captive flight loads [16]. The same grids have been used for the present store-separation studies. The initial cloud around the aircraft consists of 2 million points and 1 million points around each missile.

A. Effect of Time Step in Trajectory Simulation

The flow computation and the trajectory simulation are decoupled over a small time steps. At each time step, the flow computation is carried out until convergence of the flowfield to reach the steady-state solution for specified missile position from the aircraft. Then, the 6-DOF solver is applied to obtain the new location of the missile from the aircraft. The selection of time step is very important because the larger time steps lead to error that accumulates over time, whereas the smaller time steps take considerably longer simulation time for various trajectory-simulation cases. The time steps of 10, 50, and 100 ms are considered in the simulation of missiles separating from the aircraft at Mach number 0.6 and angle of attack (α) 0 deg. The relative linear (x, y, z along three coordinate directions), angular displacements (Euler angles ϕ, θ, ψ) and body angular rates (p, q, r about roll, pitch, and yaw axis) of the missile with time are shown in Figs. 5–7. The history of linear displacements in all three coordinate directions has no influence on the time step. The Euler angles and the body angular rates are nearly the same for both time steps of 10 and 50 ms, but deviation is very high with 100 ms time step. Therefore, further simulations have been carried out using a time step of 50 ms.

B. Effect of Skin Friction

The simulations have been carried out at Mach number 0.8 and angle of attack 10 deg with and without considering the skin-friction forces. The surface properties obtained with inviscid simulations are used as boundary-layer-edge conditions in calculating the

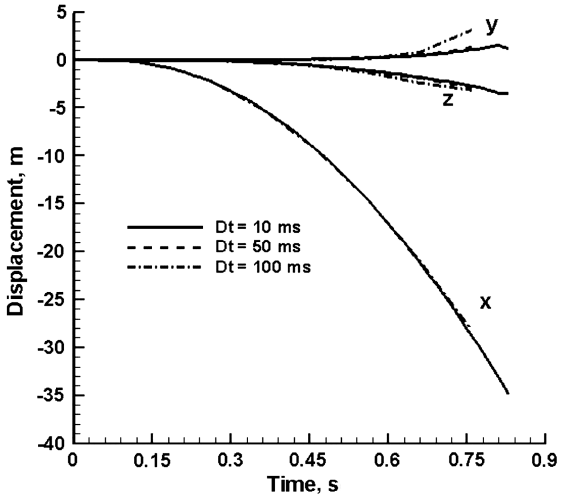

Fig. 5 Linear displacement of missile from aircraft with different time steps ($M_\infty = 0.6, \alpha = 0$ deg).

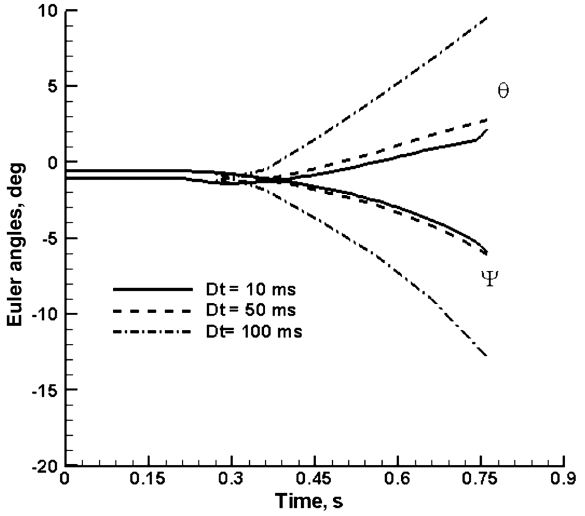

Fig. 6 Angular displacement of missile from aircraft with different time steps ($M_\infty = 0.6, \alpha = 0$ deg).

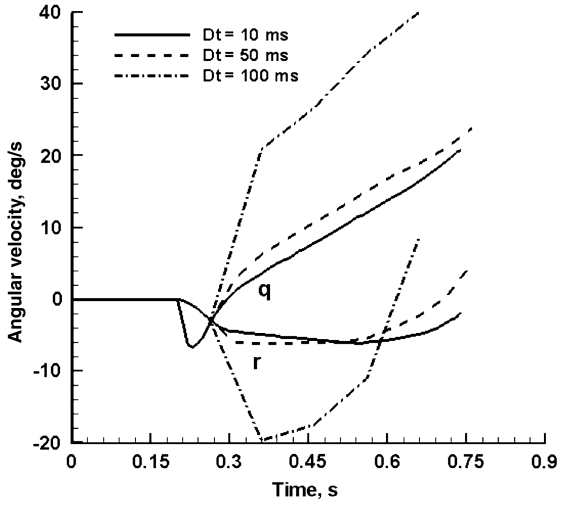

Fig. 7 Angular velocity of missile with different time steps ($M_\infty = 0.6$, $\alpha = 0$ deg).

skin-friction forces using van Driest method. The skin friction is expected to contribute significantly to the axial force, and in turn, axial displacement. The linear displacement of the missile with time is shown in Fig. 8. As expected, the axial displacement of a missile

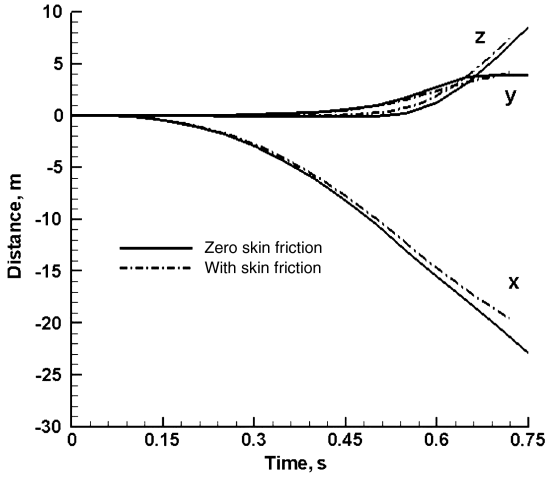

Fig. 8 Linear displacement of missile from aircraft with and without skin friction ($M_\infty = 0.8, \alpha = 10$ deg).

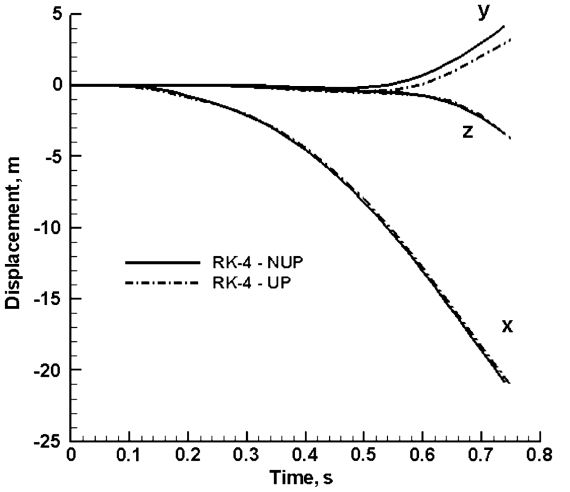

Fig. 9 Linear displacement of missile from aircraft with and without aerodynamic update ($M_\infty = 1.1, \alpha = 10$ deg).

with skin-friction force is reduced slightly compared to that of a missile without skin force. There is not much change in other trajectory variables due to skin friction. But the increase in computation time to include the skin-friction force computation is only marginal, and therefore, all the simulations are carried out with skin-friction forces.

C. Evaluation of Aerodynamic Forces in the Trajectory-Simulation Steps

The missile linear and angular accelerations due to aerodynamic, gravity, launcher and thrust forces are integrated to get the trajectory of the missile using fourth-order Runge-Kutta (RK4) method. The above forces have to be evaluated at every step of RK4. It implies that all the forces have to be evaluated four times for every time step of trajectory simulation. Among the various forces, the aerodynamic-force evaluation is computationally expensive due to connectivity regeneration and flow simulation. Instead of updating aerodynamic force at every step of RK4, the aerodynamic force in the body-axis system can be assumed to be constant during a time step. Therefore, the aerodynamic forces have to be evaluated only once at every time step, but other forces are computed at every step of RK4. The missile separation has been carried out at Mach number 1.1 and angle of attack 10 deg using both approaches of updating aerodynamic force at every step of RK4 (RK4-UP) and updating only at the beginning of RK4 (RK4-NUP). The relative linear and angular displacements of the missile with respect to aircraft are shown in Figs. 9 and 10. The results indicate that there is not much difference between the

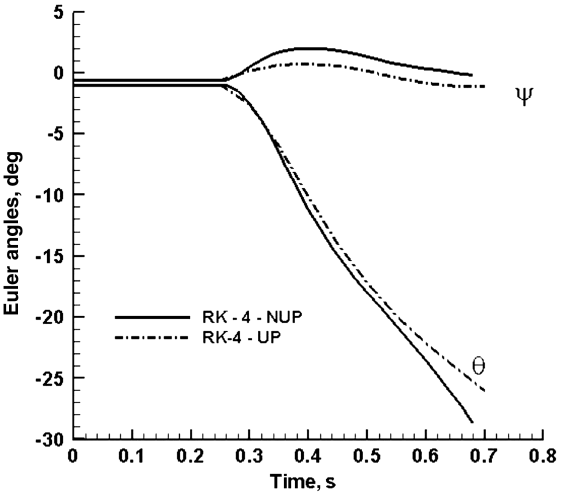

Fig. 10 Angular displacement of missile from aircraft with and without aerodynamic update ($M_\infty = 1.1, \alpha = 10$ deg).

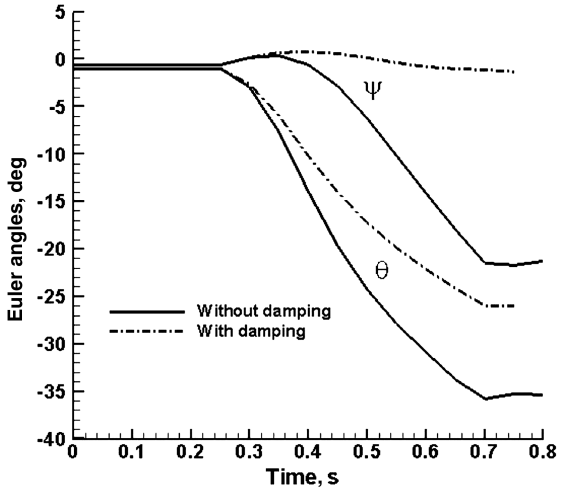

Fig. 11 Angular displacement of missile from aircraft with and without aerodynamic damping ($M_\infty = 1.1, \alpha = 10$ deg).

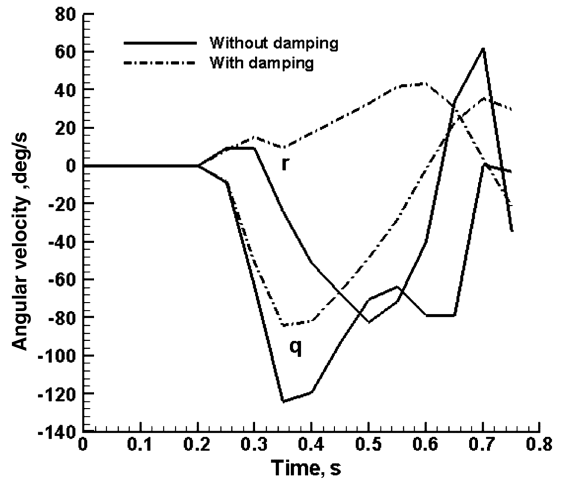

Fig. 12 Angular rates of missile with and without aerodynamic damping ($M_\infty = 1.1, \alpha = 10$ deg).

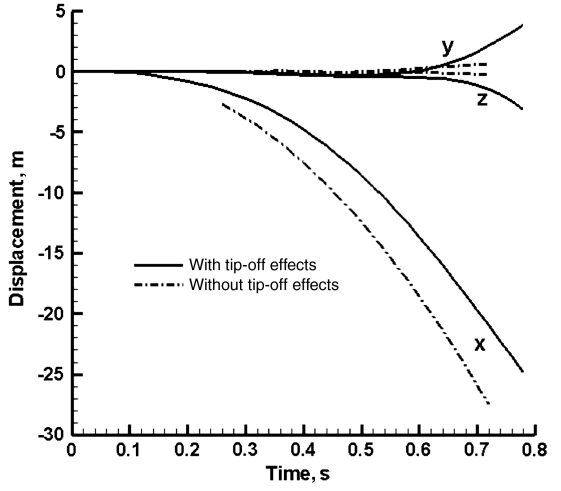

Fig. 13 Linear displacement of missile from aircraft with and without tip off ($M_\infty = 1.1, \alpha = 10$ deg).

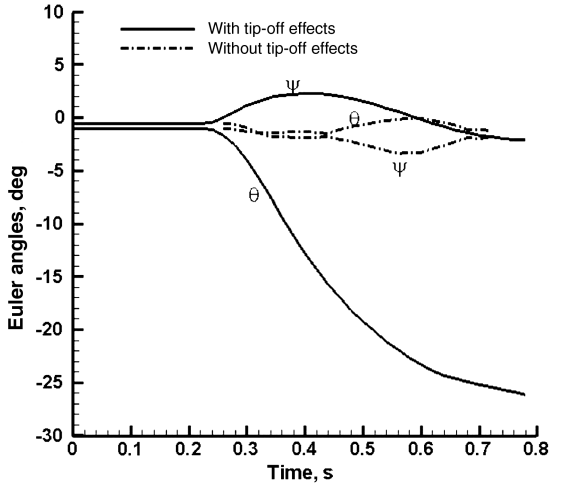

Fig. 14 Angular displacement of missile from aircraft with and without tip off ($M_\infty = 1.1, \alpha = 10$ deg).

trajectories obtained using both approaches. Therefore, further simulations have been carried out using the RK4-NUP method, and this procedure reduces the computational time by one-fourth.

D. Effect of Aerodynamic Damping

The effect of relative motion of the missile and aerodynamic damping are modeled using the transpiration boundary condition. The modeling of aerodynamic damping is felt necessary because the missile is high-lift and large-tail configuration. The trajectory has been simulated at Mach number 1.1 and angle of attack 10 deg with and without aerodynamic damping. The angular displacement and angular body rates are shown in Figs. 11 and 12. The body rates, in turn angular displacements are considerably reduced by the aerodynamic damping. The effect of aerodynamic damping is significant, and the results substantiate the implementation of the aerodynamic damping in the solver.

E. Effect of Tip-Off During Launch

The tip-off is an important phenomenon that should be considered in the modeling of powered missile launch. The trajectory simulation has been carried out including the motion in the rail and tip-off of missile when only the third launch shoe is in the rail. The missile trajectory is also simulated without rail motion, i.e., the motion of the missile until the third launch shoe leaves the rail has been simulated using a single degree of freedom with only thrust force, and from there, the coupled 6-DOF simulation has been carried out. Both trajectory simulations have been carried out at Mach number 1.1 and angle of attack 10 deg, linear and angular displacements are shown in Figs. 13 and 14. The missile takes considerably more time to leave the rail due to frictional force between the rail and the launch

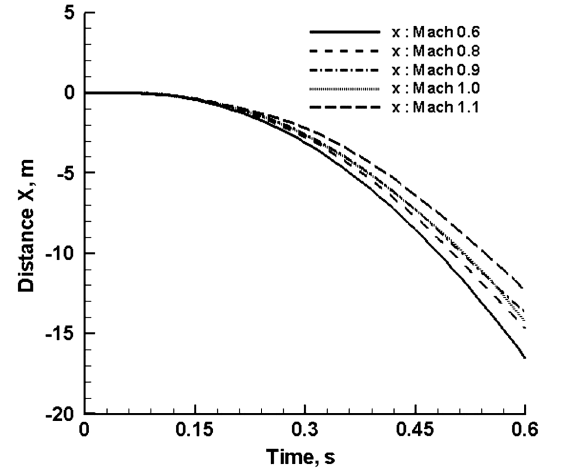

Fig. 15 Axial displacement of missile from aircraft at various freestream Mach number ($\alpha = 10$ deg).

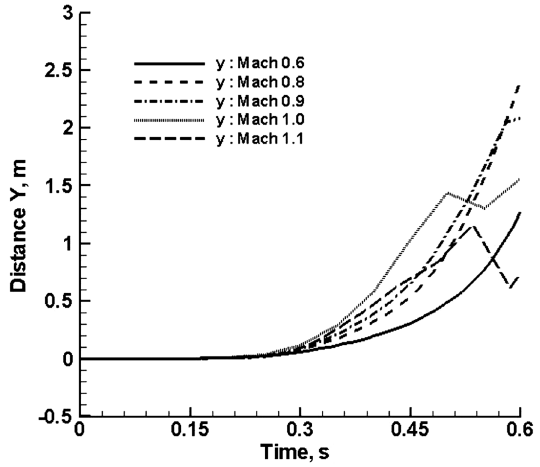

Fig. 16 Lateral displacement of missile from aircraft at various freestream Mach number ($\alpha = 10$ deg).

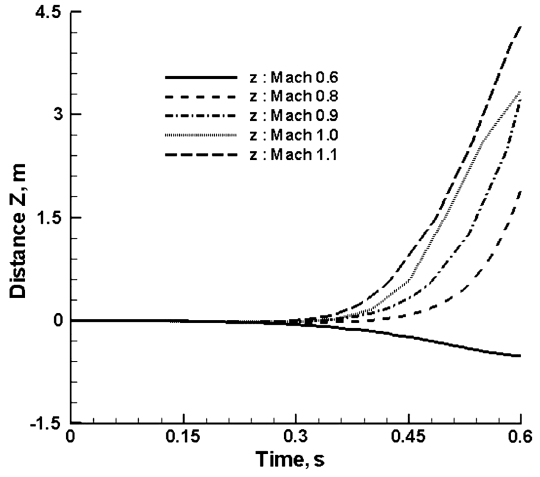

Fig. 17 Vertical displacement of missile from aircraft at various freestream Mach number ($\alpha = 10$ deg).

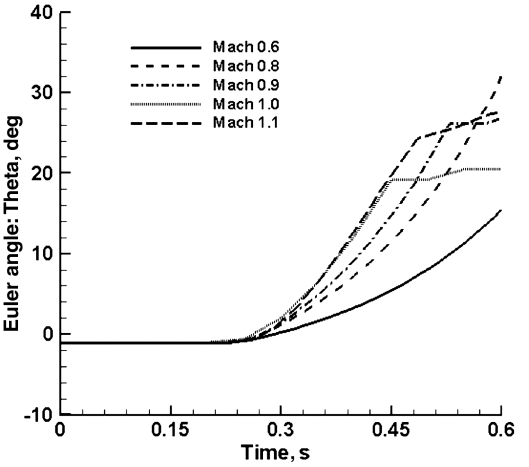

Fig. 18 Pitch angle of missile at various freestream Mach number ($\alpha = 10$ deg).

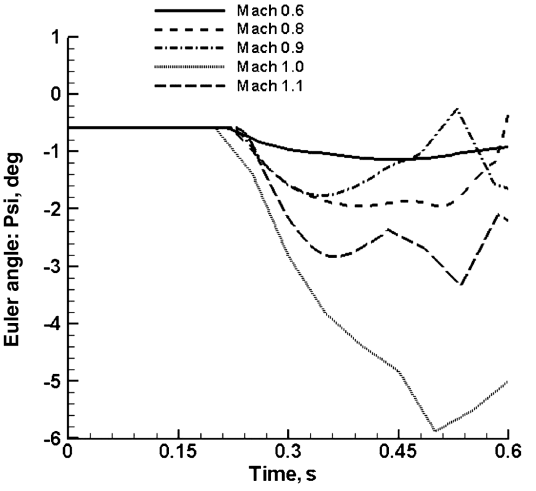

Fig. 19 Yaw angle of missile at various freestream Mach number ($\alpha = 10$ deg).

shoes compared to the simulation without considering the reaction forces. Except this initial difference, the linear displacement is the same in both the simulations, but there are considerable initial displacements in Euler angles due to tip-off effects that continuously increase further with time.

F. Applications

The separation dynamics of missiles have been carried out at Mach numbers 0.6, 0.8, 0.9, 1.1 and angle of attack 10 deg. The results of separation of inboard missile from the aircraft are presented. The linear displacements of the missile are given in Figs. 15–17. The

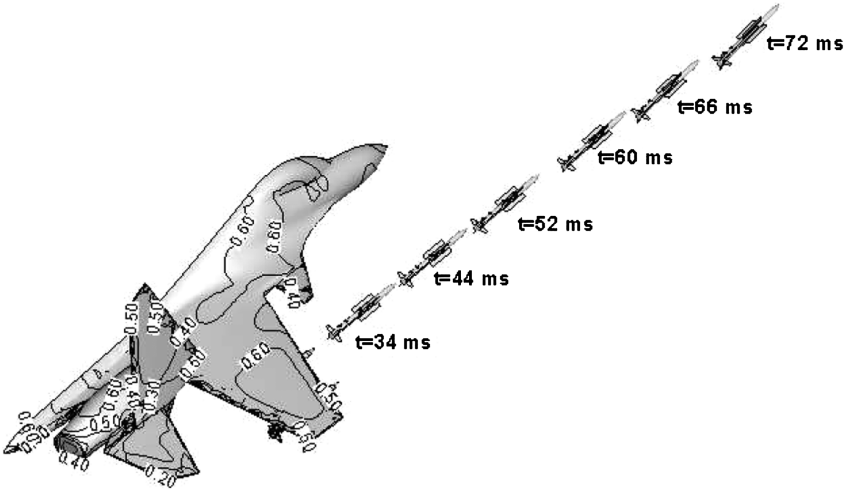

Fig. 20 Surface Mach contours and the trajectory of missile ($M_\infty = 0.6, \alpha = 10$ deg).

forces increase with the freestream Mach number due to higher dynamic pressure. The axial displacement decreases due to an increase in drag force, whereas lateral and vertical displacements increase with Mach number due to increase in lateral and normal forces. The missile traverses nearly 15 m in 600 ms in the axial direction, maximum of 2.5 and 4.5 m in the lateral and vertical directions, respectively. The missile moves away from the aircraft in the lateral direction and moves up in the vertical direction at all Mach numbers indicating the safe separation of missile for all the cases considered. The angular displacements are shown in Figs. 18 and 19. Similar to the linear displacements, the pitch and yaw angles are also increasing with Mach number. Because the missile is inherently unstable and the autopilot is not modeled in the simulation, the angles are increasing with time. At higher Mach numbers, after 450 ms, the lateral linear and angular displacement decreases. But by that time, the missile has traveled about 10 m in the axial direction. The surface Mach contours and missile trajectory are shown in Fig. 20. The trajectory clearly indicates the safe separation of the missile even without the missile control.

VII. Conclusions

The separation-dynamics study has been carried out for an air-to-air missile from a fighter aircraft using a grid-free Euler solver. The chimera cloud of points is used to get the distribution of points and connectivity. The various parameters have been considered for the simulation. The time step of 50 ms has been considered for the simulation. The importance of modeling of tip-off motion and aerodynamic damping has been brought out for the rail-launched missile application. It is also observed that updating of aerodynamic force at the beginning of time step is sufficient for such applications. The simulations at various Mach numbers indicate the safe separation of the missile, which is expected to perform better with autopilot model.

Acknowledgments

The authors thank the Director DRDL and Project Director for their support and encouragement during the work and extend their sincere gratitude to Deputy Project Director and his team for technical discussions and also for providing CAD model of the missile and fighter aircraft.

References

[1] Obermark, J., "Verification of Simulation Results Using Scale Model Flight Test Trajectories," U.S. Army Research, Development, and Engineering Command TR AMR-AE-04-01, Redstone Arsenal, AL, May 2004.

[2] Gargon, F., Taravel, P., and Raffin, J.C., "Recent Developments in Captive Trajectory Systems of the ONERA Modane Wind Tunnels," AIAA Paper 2001-0579, Jan. 2001.

[3] Murman, S. M., Aftosmis, M. J., and Berger, M. J., "Simulations of Store Separation from an F/A-18 with a Cartesian Method," *Journal of Aircraft*, Vol. 41, No. 4, 2004, pp. 870–878. doi:10.2514/1.473

[4] Nichols, R. H., and Tramel, R. W., "Application of a Highly Efficient Numerical Method for Overset-Mesh Moving-Body Problems," AIAA Paper 97-2255, June 1997.

[5] Panagiotopoulos, E. E., and Kyparissis, S. D., "CFD Transonic Store Separation Trajectory Predictions with Comparison to Wind Tunnel Investigations," *International Journal of Engineering*, Vol. 3, No. 6, 2010, pp. 538–553.

[6] Veazey, D. T., "Current AEDC Weapons Separation Testing and Analysis to Support Flight Testing," AIAA Paper 2004-6847, Nov. 2004.

[7] Bamber, M. J., "Store Separation Investigations by Grid Method Using Wind Tunnel Data," David Taylor Model Basin, Rept. 2202, April 1966.

[8] Batina, J. T., "A Gridless Euler/Navier-Stokes Solution Algorithm for Complex Aircraft Applications," AIAA Paper 1993-0333, Jan. 1993.

[9] Lohner, R., Sacco, C., Onate, E. O., and Idelsohn, S., "A Finite Point Method for Compressible Flow," *International Journal for Numerical Methods in Engineering*, Vol. 53, 2002, pp. 1765–1779. doi:10.1002/(ISSN)1097-0207

[10] Deshpande, S. M., Ghosh, A. K., and Mandal, J. C., "Least Squares Weak Upwind Methods for Euler Equations," Fluid Mechanics Rept. No. 1989-FM-1, Dept. of Aerospace Engineering, IISc, Bangalore, India, 1989.

[11] Praveen, C., and Deshpande, S. M., "Kinetic Meshless Method," Fluid Mechanics Rept. No. 2003-FM-10, Dept. of Aerospace Engineering, IISc, Bangalore, India, 2003.

[12] Anandhanarayanan, K., Nagarathinam, M., and Deshpande, S. M., "Development and Applications of A Grid-free Kinetic Upwind Solver to Multi-body Configurations," AIAA Paper 2005-4628, June 2005.

[13] More, R. R., Srinivasa Raju, S., Anandhanarayanan, K., and Krishnamurthy, R., "Nose Panel Opening Study of a Hypersonic Launch Vehicle," *Proceedings of the 1st International Conference on High Speed Transatmospheric Air & Space Transportation*, Aeronautical Society of India , Hyderabad, India, June 2007, pp. 171–177.

[14] Anandhanarayanan, K., "Development and Applications of a Gridfree Kinetic Upwind Solver to Multibody Configurations," Ph.D. Thesis, Aerospace Enginering, Indian Inst. of Science, Bangalore, India, 2003.

[15] Harish, G., Pavanakumar, M., and Anandhanarayanan, K., "Store Separation Dynamics Using Grid-Free Euler Solver," AIAA Paper 2006-3650, June 2006.

[16] Shah, V., More, R. R., Raju, S., Anandhanarayanan, K., Krishnamurthy, R., and Chakraborty, D., "Estimation of Captive Flight Loads Using Grid-Free Euler Solver," *Journal of Aircraft*, Vol. 48, No. 4, 2011, pp. 1273–1279. doi:10.2514/1.C031261

[17] Ghosh, A. K., and Deshpande, S. M., "Least Squares Kinetic Method for Inviscid Compressible Flows", *AIAA 12th CFD Conference*, San Diego, CA, June 1995;also AIAA 95-1735.

[18] Mandal, J. C., and Deshpande, S. M., "Kinetic Flux Vector Splitting for Euler Equations," *Computers & Fluids Journal*, Vol. 23, No. 2, 1994, pp. 447–478. doi:10.1016/0045-7930(94)90050-7

[19] Deshpande, S. M., "Meshless Method, Accuracy Symmetry Breaking, Upwinding, and LSKUM," Fluid Mechanics Rept. No. 2003-FM-1, Dept. of Aerospace Engineering, IISc, Bangalore, India, 2003.

[20] Deshpande, S. M., Anandhanarayanan, K., Praveen, C., and Ramesh, V., "Theory and Applications of 3-D LSKUM Based on Entropy Variables," *International Journal for Numerical Methods in Fluids*, Vol. 40, 2002, pp 47–62. doi:10.1002/(ISSN)1097-0363

[21] Ramesh, V., "Least Squares Grid-Free Kinetic Upwind Method," Ph.D. Thesis, Indian Inst. of Science, Bangalore, India, 2001.

[22] Anandhanarayanan, K., Nagarathinam, M., and Deshpande, S. M., "An Entropy Variable-Based Grid-free Euler Solver with LU-SGS Accelerator," *24th Congress of International Council of the Aeronautical Sciences*, Yokohama, Japan, 2004;also ICAS Paper 2004-2.4.3.

[23] Anandhanarayanan, K., Nagarathinam, M., and Deshpande, S. M., "Parallelisation of a Gridfree Kinetic Upwind Solver," AIAA Paper 2005-4628, June 2005.

[24] Oktay, E., and Asma, C. O., "Drag Prediction with an Euler Solver at Supersonic Speeds," AIAA 2000-0392, Jan 2000.

[25] Meakin, R. L., "Composite Overset Structured Grids," *Handbook of Grid Generation*, edited by Thompson, J. F., Weatherill, N. P., and Soni, B., CRC Press, Boca Raton, 1999, pp. 11.1–11.20.

[26] Stokes, S., Chappell, J.A., and Leatham, M., "Efficient Numerical Store Trajectory Prediction for Complex Aircraft/Store Configurations," AIAA Paper 99-3712, June 1999.